Science of the Total Environment 865 (2023) 161252

Contents lists available at ScienceDirect

Science of the Total Environment

journal homepage: www.elsevier.com/locate/scitotenv

Activation methods increase biochar's potential for heavy-metal adsorption and environmental remediation: A global meta-analysis

Abhijeet Pathy [a,b], Prem Pokharel [a], Xinli Chen [a], Paramasivan Balasubramanian [c], Scott X. Chang [a,b,*]

[a] Department of Renewable Resources, University of Alberta, Edmonton, Alberta, Canada
[b] Land Reclamation International Graduate School, University of Alberta, Edmonton, Alberta, Canada
[c] Agricultural and Environmental Biotechnology Group, Department of Biotechnology and Medical Engineering, National Institute of Technology, Rourkela, Odisha, India

HIGHLIGHTS

- Biochar's heavy metal adsorption was improved more by pre- than by post-pyrolysis activation.
- Chemical activation was most effective in enhancing biochar's adsorption of heavy metals.
- Activation by metal oxides/salts was most effective in enhancing heavy metal adsorption.
- The effect of activation depends on conditions for biochar production and adsorption.
- Activation effects on heavy metal adsorption depends on biochar's physicochemical properties.

GRAPHICAL ABSTRACT

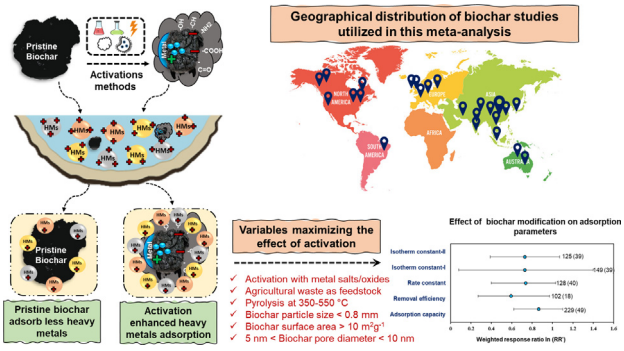

ARTICLE INFO

Editor: Daniel CW Tsang

Keywords:
Chemical activation
Particle size
Physical activation
Post-pyrolysis
Pre-pyrolysis
Removal efficiency

ABSTRACT

Removal of heavy metals (HMs) by adsorption on biochar's surface has shown promising results in the remediation of contaminated soil and water. The adsorption capacity of biochar can be altered by pre- or post-pyrolysis activation; however, the effect of activation methods on biochar's adsorption capacity varies widely. Here, we conducted a meta-analysis to identify the most effective methods for activation to enhance HM removal by biochar using 321 paired observations from 50 published articles. Activation of biochar significantly improves the adsorption capacity and removal efficiency of HMs by 136 and 80 %, respectively. This study also attempts to find suitable feedstocks, pyrolysis conditions, and physicochemical properties of biochar for maximizing the effect of activation of biochar for HMs adsorption. Activation of agricultural wastes and under pyrolysis temperatures of 350–550 °C produces biochars that are the most effective for HM adsorption. Activation of biochars with a moderate particle size (0.25–0.80 mm), low N/C (<0.01) and H/C ratios (<0.03), and high surface area (> 100 $m^2\ g^{-1}$) and pore volume (> 0.1 $cm^3\ g^{-1}$) are the most desirable characteristics for enhancing HM adsorption. We conclude that pre-pyrolysis activation with metal salts/oxides was the most effective method of enhancing biochar's potential for adsorption and removal of a wide range of HMs. The results obtained from this study can be helpful in choosing appropriate methods of activations and the suitable choice of feedstocks and pyrolysis conditions. This will maximize HM adsorption on biochar surfaces, ultimately benefiting the remediation of contaminated environments.

1. Introduction

Rapid industrialization has disturbed the ecological balance and dramatically increased the contamination of the environment with toxic

* Corresponding author at: Department of Renewable Resources, University of Alberta, Edmonton, Alberta, Canada.
E-mail address: sxchang@ualberta.ca (S.X. Chang).

http://dx.doi.org/10.1016/j.scitotenv.2022.161252
Received 29 August 2022; Received in revised form 23 December 2022; Accepted 24 December 2022
Available online 30 December 2022

pollutants such as heavy metals (HMs). Heavy metals are discharged from effluents of various industries such as mining, ceramic making, electroplating, battery manufacturing, metal finishing, glass production, and leather processing (Zamora-Ledezma et al., 2021). Due to their potential for bioaccumulation, high toxicity and carcinogenicity, HMs are hazardous pollutants posing severe threats to the environment and human health. Heavy metals can also form complexes and coexist with complexing agents such as ethylene diamine tetraacetic acid, escalating their toxicity and environmental damage (Ore and Adeola, 2021). Thus, removing HMs from contaminated soil and water is essential for environmental protection and human health.

Heavy metals can be removed from soil and water through adsorption, electrocoagulation, flotation, ion exchange, phytoremediation, packed bed filtration, and reverse osmosis (Rajendran et al., 2022). Adsorption is a simple method for HM immobilization, and the appropriate adsorbent can effectively remediate contaminants. Adsorbents can be produced from abundant natural resources, such as agricultural residues, forest residues, and municipal wastes (Chai et al., 2021). Biochar, a carbon-rich, porous material produced by the thermal decomposition of organic materials in an oxygen-limited environment. Biochar has been found to be an effective adsorbent for HM removal from soil and water (El-Naggar et al., 2022). The immobilization of HMs on biochar can also occur via surface redox reactions, catalytic degradation, and precipitation, in addition to adsorption (He et al., 2022). The dominant immobilization mechanism may vary depending on the HMs targeted. For instance, when alkaline biochars are utilized, HMs such as Cd and Pb are precipitated and immobilized on the surface of the biochar (Chi et al., 2017). Similarly, redox-sensitive HMs such as Cr and As undergo reduction (for Cr) and oxidation (for As) prior to immobilization on the biochar surface, depending on the elemental and functional groups present in the biochar (Xu et al., 2022). In aqueous solutions, biochar efficiently absorbs organic and inorganic contaminants, including HMs (Ambaye et al., 2020; Barquilha and Braga, 2021). The ability of biochar to remove pollutants is contingent on its physical and chemical properties, which are affected by feedstock type, pyrolysis temperature, heating rate, and residence time (Nzediegwu et al., 2021b).

Biochar's physicochemical properties (porosity, specific surface area, and surface functional groups) as well as adsorption capacity can be enhanced by activation. Depending on the process used, physical, chemical, or biological activation methods may be employed. Commonly used physical activation techniques include exposure to an oxidising medium (steam, carbon dioxide, ozone, or air), size reduction through ball milling, activation through radiation (microwave heating, plasma radiation, and electrochemical heating), and ultrasonic agitation (Akhil et al., 2021; Bardestani and Kaliaguine, 2018; Kawi and Kathiraser, 2015). Physical activations enhance the mesopore and micropore architectures of biochar, thereby enhancing its adsorption capacity. Biochar is chemically activated with acids, alkalis, metal oxides, organic solvents, and polymers. Chemical activation increases biochar's surface area, cation exchange capacity, and adsorbable functional groups (Leng et al., 2021). By anaerobically digesting biomass, microbes increase the cation/anion exchange capacity and surface area of biochar. Following pyrolysis, microbes can alter the biochemical characteristics of biochar (Kazemi Shariat Panahi et al., 2020; Yuvaraj et al., 2021). Whether activation occurs before or after pyrolysis influences the properties of biochar. Biochar can be activated prior to (pre-pyrolysis) or after pyrolysis (post-pyrolysis). Improvements in biochar's physicochemical properties help biochars to adsorb more HMs through cation exchange, physical adsorption, and electrostatic attraction (Mariana et al., 2021).

Previous studies have reported positive (Li et al., 2017), negligible (Arabyarmohammadi et al., 2018; Fahmi et al., 2018), or even negative (Wu et al., 2016; Zhang et al., 2018b) effects of biochar on pollutant removal. The different findings of biochar in removing pollutants could also result from the effect of activations, such as the use of different types of activations, on the biochar's physical and chemical properties (Nzediegwu et al., 2021a). A quantitative synthesis of results across multiple studies might assist in determining the overall effects of biochar on pollutant removal and identify sources of variation (Gurevitch et al., 2018). Not all activation processes enhance biochar adsorption of HMs. Gao et al. (2018) found that ammonium chloride as an activation agent decreased the Cu adsorption capacity of biochars (Gao et al., 2018). Similarly, activation with lignin decreased the Cd adsorption capacity of corn cob biochars (Luo et al., 2018). The effectiveness of biochar activation also depends on the chemical properties of the pollutant. Acid activation may be effective at eliminating anionic contaminants but not all HMs (as, in general, HMs are present as cations). The physicochemical properties of biochars activated prior to pyrolysis can vary from those activated after pyrolysis (Mahdi et al., 2019). Therefore, it is essential to comprehend which activation technique is desirable for enhancing the adsorption of HMs by biochars.

Selecting the proper feedstock type, production condition, and activation method will aid in the success of remediation projects. Heavy metal adsorption on biochar has been summarised in several reviews. This study quantified the impact of activation techniques on HM adsorption by biochar. This study quantified the impact of biochar's physicochemical properties on the adsorption process for HMs. A meta-analysis studies primary literature data statistically and synthesises quantitative estimates of the investigated phenomenon (Mikolajewicz and Komarova, 2019). By providing a more precise treatment effect estimate, meta-analysis enhances the generalizability of individual study findings. This could be misleading by compounding the bias in each individual study; therefore, it is essential to include studies that are free of error and bias (Wiernik and Dahlke, 2020). Meta-analysis can be used to comprehend how biochar activation influences the adsorption of HMs.

To the best of our knowledge, no previous research has analyzed the impact of activation methods on biochar's HM adsorption using meta-analysis. In this study, we performed a meta-analysis with the following objectives: (1) to determine how different types of activation methods impact biochar's HM adsorption, and (2) to understand how activation effect is dependent on biochar's physical and chemical characteristics, pyrolysis temperature, and experimental conditions in enhancing the adsorption of HMs on activated biochar. The results of this study will help identify suitable activation methods and biochar properties for improving the efficiency of HM adsorption, benefiting the remediation of contaminated environments.

2. Materials and methods

2.1. Literature search

A literature search was conducted to collect data for this meta-analysis from peer-reviewed articles published between 2009 and August 2021. The SCOPUS and GOOGLE SCHOLAR databases were searched using various keyword combinations: (char OR biochar OR activated biochar OR modified biochar OR engineered biochar) AND (physical activation OR chemical activation OR biological activation OR novel activation) AND (adsorption OR removal OR remediation) AND (heavy metals OR metals OR metal ions OR heavy metal contamination OR metal pollutants). A total of 136 research articles were collected using these search terms. The following criteria were used for data to be included in this meta-analysis: (1) the study reported the sample size, (2) adsorption studies with a treatment effect (activation of biochar) paired with a control (pristine biochar) in the same set of experimental conditions, and (3) studies reporting at least one of the following adsorption parameters: (a) adsorption capacity, (b) adsorption removal efficiency, (c) rate constant of the adsorption kinetics, and (d) two isotherm constants associated with isotherm equations. Studies that reported biochar combined with any other adsorbents for remediating HMs were excluded. Moreover, articles with missing units for any of the above-mentioned adsorption parameters were excluded. If multiple adsorbents were used in the experiment, only the data for biochar were collected. The authors of some articles were contacted to obtain additional information such as the unit, sample size, missing standard error (SE) or standard deviation (SD) in the data.

2.2. Data collection

A total of 50 articles met the criteria described above and were selected to extract the data used in this meta-analysis. The dataset includes mean values with the number of replications (n) and the standard error (SE), or standard deviation (SD) obtained from tables, figures and supplementary materials of the published articles. The "graph reader" (http://www.graphreader.com/), a free online software, was used for extracting the mean and SE or SD data from figures. For studies that reported SD but not SE, the latter was calculated using Eq. (1):

$$SE = SD/\sqrt{n} \quad (1)$$

If the experimental value for maximum adsorption capacity was not reported, it was calculated by solving the kinetics equation of adsorption. The information related to feedstock type, pyrolysis condition, pristine biochar properties, experimental adsorption condition (such as temperature, pH, contact time for adsorption), activation type (pre/post-pyrolysis), and mode of activation (activation using physical/chemical/ biological methods) were also extracted from the articles. A total of five adsorption parameters (adsorption capacity, HM removal efficiency, rate constant of the adsorption kinetics, and two isotherm constants) that represent the overall adsorption process were considered as "the dependent variables" to evaluate biochar's HM adsorption potential. Most of the adsorption studies included in this analysis were reported to fit well either with pseudo-first-order or pseudo-second-order kinetics. Thus, the kinetics constant of our model is associated with pseudo-first-order or pseudo-second-order kinetics. The adsorption data collected for the dependent variables "isotherm constant 1" (IC-I) and "isotherm constant 2" (IC-II) follow either the Langmuir or the Freundlich isotherm model. The IC-I represents the Langmuir constant (for adsorption data that follow the Langmuir isotherm) and the Freundlich adsorption capacity (K_f) (for adsorption data that follow the Freundlich isotherm). The IC-II represents the maximum adsorption capacity for the adsorption data following the Langmuir isotherm and "n" for the adsorption following the Freundlich isotherm. The targeted HMs included in this analysis are As, Pb, Cu, Cd, Cr, Ni, and Hg. Almost all the adsorption experiments using engineered biochars were carried out at a bench scale. Thus, unlike in the soil or aquatic system, the HMs included in this analysis are based on a single oxidation state.

Biochar feedstock type, pyrolysis condition (highest heating temperature, heating rate, and residence time), activation (type and mode of activation), and experimental adsorption condition (temperature, pH, and duration) were selected as independent variables. Independent variables were categorized into groups to facilitate the analysis and identify the major factors affecting biochar's HM adsorption potential. Biochar feedstocks were categorized into agricultural waste (such as rice straw, corn straw, peanut shell, coconut shell, and sugarcane bagasse), grass biomass, and woody biomass (such as pine dust, hickory, softwood chips, and sawdust). Biochar size was classified into three groups: fine (< 0.25), medium (0.25–0.83), and coarse (> 0.83 mm). The particle size classification (fine, medium, and coarse) was adopted from a study which discussed the influence of biochar particle size on soil and water properties (Liu et al., 2017). Pyrolysis temperature was categorized into low (< 350), medium (350–550), high (550–700), and very high (>700 °C). The categorization of temperature was adopted from a recent meta-analysis (Pokharel et al., 2020). It is important to note that activation, such as thermal activation, uses high temperature as their activation technique; however, the activation (heating at very high temperature) occurs as an additional step, and the temperature used for heating at the first step was considered as the pyrolysis temperature. The impact of pyrolysis temperature on HMs adsorption was determined from the data that used unmodified biochar or the pyrolysis temperature used before any modification. Biochar activations were categorized based on the type of activation (pre-pyrolysis or post-pyrolysis) and mode of activation (biological, chemical and physical methods). Further, chemical activation was categorized into four groups: acid, alkali, metal, and others (such as hydrogen peroxides, silicate, and polymers). Similarly, the pH of the solution was classified into three groups: <5 (acidic), 5–8, and > 8 (alkaline); the categorization was done based on the metal's speciation at different pH ranges (Essington, 2015). The adsorption contact time was divided into five groups: <5, 5–8, 9–24, 25–48, and > 48 h. All the details of the collected data are provided in the supplementary table.

2.3. Data analysis

The natural log-transformed response ratio (ln RR') was used to quantify the effects of activation on biochar's adsorption for HM as follows.

$$\ln\ RR' = ln\ \left(\overline{X_t}\right)/\left(\overline{X_c}\right) \quad (2)$$

where $\overline{X_t}$ is the mean value of the adsorption parameters in the treatment group, and is the mean value of the adsorption parameters in the control group. Effect size in the meta-analysis is affected by the weight of the individual observation, which subsequently shapes the inference from the meta-analysis. In previous meta-analysis studies, various weighting functions have been used. However, it is essential to note that the use of variance estimates in those functions is often not reliable because the majority of the studies have a diverse set of experimental conditions, and the sample size was small (Ma and Chen, 2016). Several meta-analysis studies used the number of replications for estimating the weighing function (Ma and Chen, 2016; Zhang et al., 2018a). This function assigns less extreme weight and gives a lesser weight to studies having multiple non-independent observations. Eq. (3) represents the calculation for the weighing factor.

$$W_r = (N_t \times N_c)/(N_t + N_c) \quad (3)$$

Wr represents the weight associated with ln RR' of each variable, and Nt and Nc, respectively, represent the number of replications in treatment and control. The study was conducted using the maximum likelihood estimation with the lme4 package in R (4.1.3 version). The 'confint ()' function in the 'boot' package of R was used to extract the estimates of the weighted response ratio (ln RR') for generating the 95 % confidence intervals ("Package 'boot,'", 2016). The following expression was used to convert the log-transformed weighted response ratio to the percentage change (or effect size, for ease of interpretation) (Eq. (4)).

$$Effect\ Size\ (\%) = \left(e^{lnRR'} - 1\right) \times 100\% \quad (4)$$

It has been considered that the effect of activation on HMs adsorption by biochar is significantly different from the control if the 95 % confidence interval does not overlap with zero (Luo et al., 2006). The mean effect sizes among the group levels of independent variables were significantly different if their 95 % CIs did not overlap among the group levels (Chen et al., 2022).

3. Results

3.1. Overall effect of activation on biochar's adsorption properties

Activation significantly enhanced biochar's adsorption capabilities for HMs (Fig. 1; Table 1). Activation increased biochar's HM adsorption capacity and removal efficiency by 136 and 80 %, respectively, compared to the pristine biochar. Activation of biochar significantly increased the rate constant by 107 % and the adsorption isotherm constants IC-I and IC-II by 105 and 107 %, respectively. All the adsorption parameters studied were increased by the activation of biochar ($p < 0.05$).

3.2. Effect of different activation methods on biochar's adsorption characteristics

All activation methods studied in this meta-analysis enhanced biochar's adsorption properties, depending on the type (pre- or post-pyrolysis activation) and mode (chemical or physical) of activation (Table 2; Fig. 2). Pre-

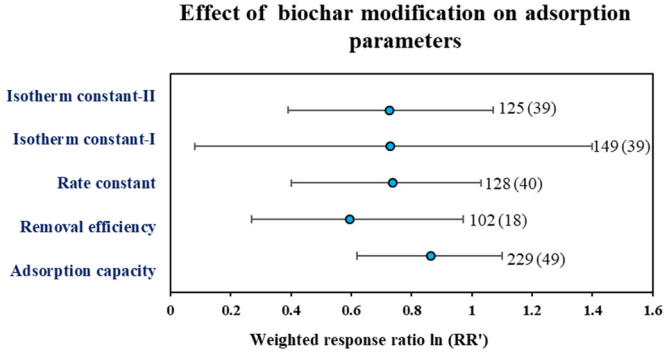

Fig. 1. Overall effect of activation of biochar on its heavy metal adsorption parameters. The bars represent 95 % confidence intervals, and the number beside each bar represents sample size with the number of studies noted in the parentheses.

and post-pyrolysis activations increased biochar's adsorption capacity by 223 and 93 %, respectively, compared with pristine biochars. However, the increase in adsorption capacity between pre-and post-pyrolysis activation was not significantly different (Fig. 2). The removal efficiency, rate constant, and isotherm constants were increased by 107, 156, and 163 %, respectively, by pre-pyrolysis activation, and by 65, 72, and 74 %, respectively, by post-pyrolysis activation (Table 2; Fig. 2). Biochar's HMs adsorption capacity was significantly increased by 157 and 38 % by chemical and physical activation, respectively, but not by biological activation. Among the chemical activation methods, metal activation was the most effective in increasing biochar's adsorption capacity, removal efficiency, rate constant, and isotherm constant, followed by alkali activation (Table 2). In contrast, acid activation did not affect those adsorption properties (Table S1).

3.3. Activation effects on biochar's HM adsorption are dependent on pyrolysis temperature, feedstock type and biochar particle size

Activation increased the adsorption capacity by 120, 151, 115, and 191 % for biochars produced at temperatures of <350, 350–550, 550–700, and > 700 °C, respectively, as compared to pristine biochars. The adsorption capacity among three categories of pyrolysis temperature had similar increments (Fig. 3). However, removal efficiency, rate constant and isotherm constants increased the most for activated biochars produced at 350–550 °C (Table 3; Fig. 3). Similarly, the choice of feedstock also impacted biochar's HM adsorption. Activation of biochars derived from agricultural waste and woody biomass increased the adsorption capacity by 163 and 105 %, respectively, compared to pristine biochars derived from similar feedstocks. Similarly, activation increased the removal efficiency and rate constant more for biochars derived from agricultural wastes than from woody biomass (Table 3). The effect of activation on biochar's adsorption of HMs was also dependent on the particle size of the resulting biochar. The adsorption capacity for the activated biochar having a particle size of <0.25, 0.25–0.83, and > 0.83 mm was increased by 127, 163, and 104 %, respectively, compared to pristine biochars (Table 3). The increment in adsorption capacity for different categories of biochar particle sizes was not significantly different (Fig. 3). A similar trend was observed for HM removal efficiency, rate constant, and isotherm constant (Table S2).

3.4. Activation effect on biochar's HM adsorption is dependent on biochar chemical composition

The effect of activation on biochar's HM adsorption differs with biochar's elementary composition. For instance, activation increased the adsorption capacity of biochars with a lower N/C ratio (<0.01) by 236 % (compared to pristine biochar), but by 87 % for those with a higher N/C ratio (> 0.033) (Table S3; Fig. S1). However, the increase in adsorption capacity for categorized N/C ratios was not significantly different (Fig. S1). Similarly, activation of biochars having lower O/C (<0.1) and H/C (<0.033) ratios had the highest increase in adsorption capacity; the effect decreased with increasing biochar O/C and N/C ratios. Activation increased the rate and isotherm constants more for biochars with lower than those with higher N/C, H/C, and O/C ratios (Table S3).

3.5. Activation effect on biochar's HM adsorption is dependent on biochar surface characteristics

The effect of activation on biochar HM adsorption was influenced by biochar's surface area, pore volume and diameter. For instance, activation increased the adsorption capacity of biochars with a lower surface area (<10 $m^2\ g^{-1}$) by 140 % (compared to pristine biochar), but by 215 % for biochars with a higher surface area (>100 $m^2\ g^{-1}$) (Table S4; Fig. S2). Similarly, activation increased the adsorption capacity of biochars having a pore volume in the range of 0.01–0.1 $cm^3\ g^{-1}$ by 112 % (compared to pristine biochar) but by 319 % for those with higher pore volumes (>0.1 $cm^3\ g^{-1}$). However, activation increased the adsorption capacity of biochar with a small pore diameter (< 5 nm) by 228 % but by 109 %, and 68 % (compared to pristine biochar), respectively, for biochars having a pore diameter of 5–8 nm, and > 10 nm.

Activation increased the rate constant for HM adsorption on biochars with a low surface area (< 10 $m^2\ g^{-1}$) by 145 % (compared to pristine biochar) but by 113 % for those with a high surface area (>100 $m^2\ g^{-1}$). The adsorption capacity among the various categories of biochar surface area, pore volume, and pore diameter had similar increments (Fig. S2). The activation effect on the rate constant of biochar having different pore volumes was similar to that of adsorption capacity. Activation increased the rate constant and adsorption capacity for biochars having a larger pore diameter. But the results for isotherm constant for HMs adsorption on activated biochar do not follow any particular trend (Fig. S2). The activation of biochars having pore diameters in the range of 5–10 nm had the highest increment for the isotherm constant (Table S4).

3.6. Activation effect on biochar's HM adsorption is dependent on solution pH and temperature

The effect of activation on biochar's HM adsorption was dependent on experimental conditions such as pH and adsorption contact time (Table S5; Fig. S3). For instance, activated biochars exhibited their highest adsorption capacity in the pH range of 5–8. Activation increased the adsorption capacity of biochar for adsorption by 70 % (compared to pristine

Table 1
Overall effect of activation of biochar on its adsorption properties.

Dependent variable	*P*-value	Mean (ln RR') weighted response ratio	Confidence interval		Sample size	No. of studies	Effect size (%)
			high	low			
Adsorption capacity	**<0.001***	0.86	1.10	0.62	229	49	136
Removal efficiency	**0.001**	0.59	0.97	0.27	102	18	80
Rate constant	**<0.001**	0.73	1.03	0.40	128	40	107
Isotherm constant-I	**<0.001**	0.72	1.07	0.39	149	39	105
Isotherm constant-II	**0.022**	0.73	1.40	0.08	125	39	107

* *P*-values <0.05 (highlighted with bold fonts) are statistically significant.

Table 2
Effect of different types of activations of on biochar's adsorption properties.

Dependent variable	Independent variable	Subcategory	*P* value	Effect size (%)
Adsorption capacity	Activation type	Pre-pyrolysis	**<0.001***	223
		Post-pyrolysis	**<0.001**	93
	Activation mode	Chemical	**<0.001**	157
		Physical	**0.030**	38
		Biological	0.128	123
		Acid	0.098	97
		Alkali	**0.002**	121
		Metal	**<0.001**	246
	Chemical activation	Other	**0.003**	75
Removal efficiency	Activation type	Pre-pyrolysis	**0.071**	107
		Post-pyrolysis	**0.010**	65
	Activation mode	Chemical	**0.003**	85
		Physical	NA[a]	NA
		Biological	NA	NA
	Chemical activation	Acid	0.744	25
		Alkali	**0.084**	129
		Metal	**0.034**	90
		Other	0.090	60
Rate constant	Activation type	Pre-pyrolysis	**<0.001**	156
		Post-pyrolysis	**<0.001**	72
	Activation mode	Chemical	**<0.001**	120
		Physical	0.412	19
		Biological	0.131	192
	Chemical activation	Acid	0.44	25
		Alkali	**0.010**	160
		Metal	**0.030**	156
		Other	**0.032**	60
Isotherm constant	Activation type	Pre-pyrolysis	**0.002**	161
		Post-pyrolysis	**<0.001**	76
	Activation mode	Chemical	**<0.001**	127
		Physical	0.412	19
		Biological	0.131	191
	Chemical activation	Acid	0.630	17
		Alkali	**0.010**	158
		Metal	**0.030**	156
		Other	**0.032**	66

* P-values <0.05 (highlighted with bold fonts) are statistically significant.
[a] Insufficient datasets to obtain an output.

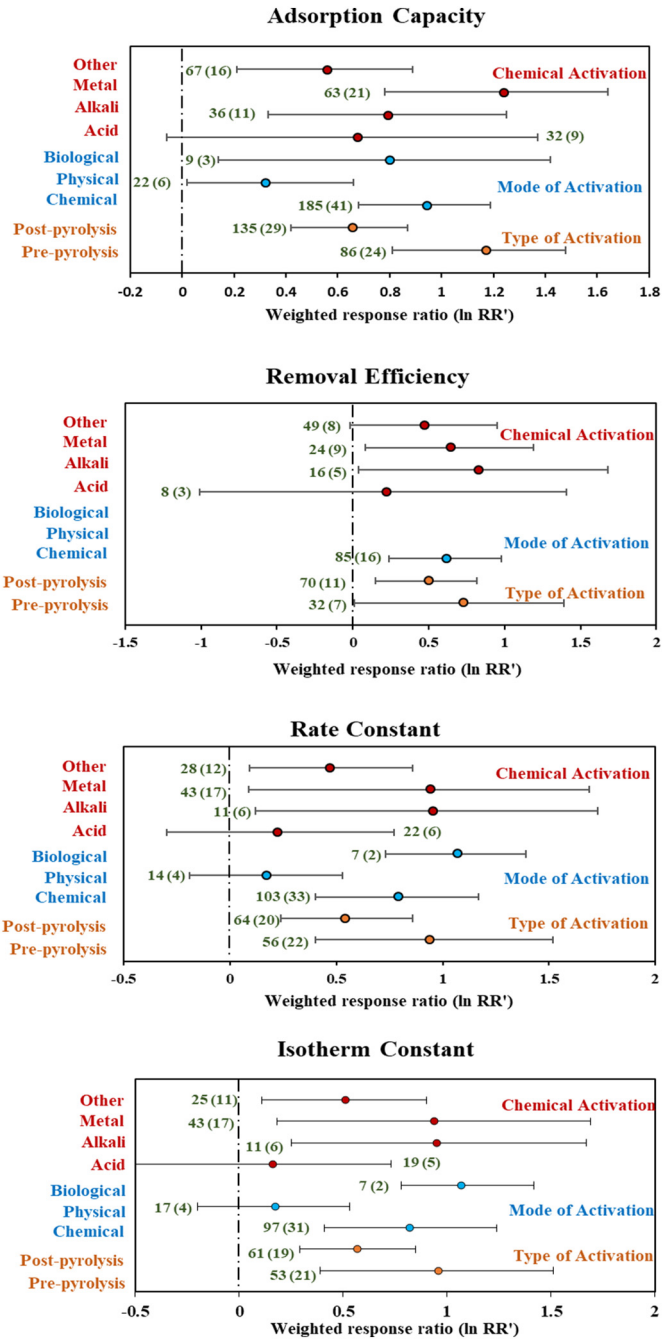

Fig. 2. Impact of different types of activation on biochar's HMs adsorption. The bars represent 95 % confidence intervals, and the number beside each bar represents sample size with the number of studies noted in the parentheses.

biochar) when pH of <5 but by 119 % when pH ranged between 5 and 8. Similarly, the adsorption capacity of activated biochar increased with the increment in contact time. The increments in adsorption capacity for different categories of pH, and adsorption temperature were not significantly different (Fig. S1). The activation effect of biochar on its HMs removal efficiency under various adsorption experimental conditions was similar to that of the results of its HMs adsorption capacity. The rate and isotherm constant for the HMs adsorption process on activated biochars increased with increasing contact time and was highest when the pH was <5 (Table S5).

4. Discussion

Our results show that the adsorption capacity, removal efficiency, rate constant, and isotherm constant of biochars for HMs adsorption were enhanced by different activation methods (Table 1). The adsorption capacity provides the amount of HMs taken up per unit mass of the adsorbent, whereas the adsorption removal efficiency indicates the quantity of adsorbate removed as a percentage of a given amount of solution. Adsorption isotherms and kinetics are crucial for determining the adsorption mechanism. Understanding the associated constants is essential for inferring the adsorption parameters of the process. The Langmuir and Freundlich isotherm models are the most frequently used in adsorption studies. The majority of the studies included in our meta-analysis fit the Langmuir and Freundlich models. The two Langmuir constants are represented by the intercept and slope of the liner plot between $1/q_e$ and $1/C_e$ (K_L and q_m). While the intercept and slope of a liner plot between ln q_e and ln C_e at a constant temperature yield the Freundlich model constants of K_f and n. Fitting the Langmuir model indicates that the monolayer saturation is at equilibrium when the surface is covered with HMs, and no further adsorption can occur (Alver and Metin, 2012). The K_L value represents the affinity of HMs for the biochar surface, while qm represents the biochar's theoretical maximum adsorption capacity. If the adsorption data fit the Freundlich model, adsorption occurs on a heterogeneous surface with interactions between adsorbed molecules (Gupta and Babu, 2009). The constant K_f of the Freundlich model represents the ease with which HMs are absorbed onto the biochar surface, whereas the value n indicates the favorability of the adsorption reaction. The adsorption reaction between HMs and biochar can be classified as irreversible ($1/n = 0$), favourable ($0 < 1/n < 1$), or unfavourable ($1/n > 1$) (Greluk and Hubicki, 2010). Both Langmuir and Freundlich models have their own assumptions and different mechanisms;

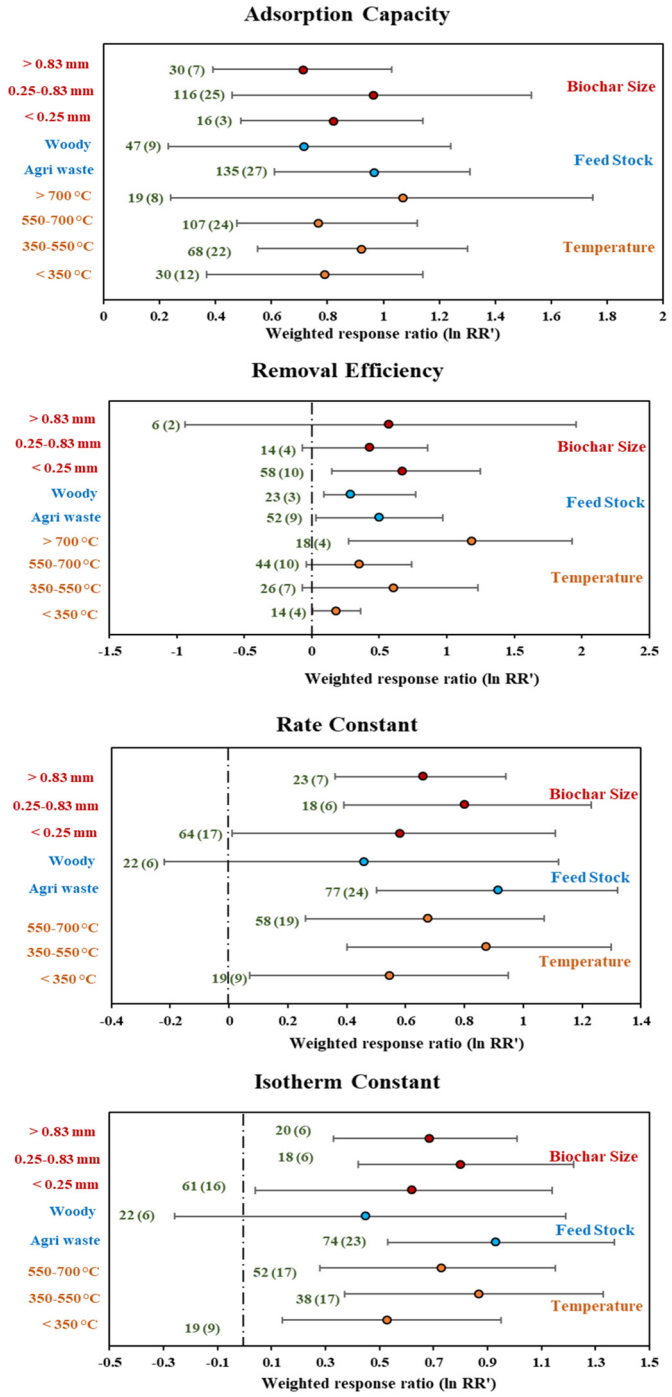

Fig. 3. Impact of biochar size, feedstock type and pyrolysis temperature on biochar's HMs adsorption. The bars represent 95 % confidence intervals, and the number beside each bar represents sample size with the number of studies noted in the parentheses.

however, the parameters that can be quantified from both models can be comparable. For instance, higher values of K_L and K_f represent higher affinity and ease of adsorption of HMs on the biochar surface. Thus, in our meta-analysis study, the K_L and K_f were represented as IC-I and the other two parameters from the two models were represented as IC-II.

Similarly, the kinetics of an adsorption reaction indicate the rate of the reaction. The reaction rate determines the contact time, and a short contact time is economically advantageous for the adsorption process. Various models can be used to determine the reaction's rate constant by fitting the adsorption data to them. The most commonly implemented kinetics are

Table 3
Impact of activation of biochar on its heavy metal adsorption under different biochar sizes, feedstock types and production temperatures.

Dependent variable	Independent variables	Subcategory	P value	Effect size (%)
Adsorption capacity	Pyrolysis temperature (°C)	< 350	**0.004***	120
		350-550	**<0.001**	151
		550–700	**<0.001**	115
		> 700	**0.020**	191
	Feedstock	Agri waste	**<0.001**	163
		Woody	**0.024**	105
	Size of biochar (mm)	< 0.25	**<0.001**	127
		0.251–0.83	**0.008**	162
		> 0.83	**0.002**	104
Removal efficiency	Pyrolysis temperature (°C)	< 350	**0.033**	19
		350–550	0.110	83
		550–700	0.110	42
		> 700	**0.063**	227
	Feedstock	Agri waste	**0.064**	64
		Woody	**<0.001**	33
	Size of biochar (mm)	< 0.25	0.022	96
		0.251–0.83	0.139	53
		> 0.83	0.579	76
Rate constant	Pyrolysis temperature (°C)	< 350	**0.046**	72
		350–550	**0.001**	139
		550–700	**0.004**	96
		> 700	0.325	119
	Feedstock	Agri waste	**<0.001**	149
		Woody	0.270	58
	Size of biochar (mm)	< 0.25	**0.055**	79
		0.251–0.83	**0.019**	122
		> 0.83	**<0.001**	93
Isotherm constant	Pyrolysis temperature (°C)	< 350	**0.047**	69
		350–550	**0.001**	138
		550–700	**0.005**	107
		> 700	**0.325**	118
	Feedstock	Agri waste	**<0.001**	153
		Woody	0.270	56
	Size of biochar (mm)	< 0.25	**0.050**	85
		0.251–0.83	**0.019**	122
		> 0.83	**<0.001**	98

* P-values <0.05 (highlighted with bold fonts) are statistically significant.

pseudo-first order and pseudo-second order kinetics. The majority of the studies included in our meta-analysis reported rate constant data that were fitted to pseudo-first-order and pseudo-second-order models. According to a fit to a pseudo-second-order model, the primary interaction forces between HMs and biochar are covalent forces and ion exchange reactions. In short, a pseudo-second-order reaction is an ideal fit for chemisorption as the dominant mechanism (Alver and Metin, 2012). Other kinetics models can be fitted; however, the data reported by the studies included in our meta-analysis were insufficient to fit other kinetics models; hence, discussing them is outside the scope of this study.

The magnitude of the increment varies widely with the type and mode of activation, feedstock type and pyrolysis temperature used for biochar production, and the particle size of the produced biochar. Moreover, the increment was also affected by the adsorption temperature, solution pH, biochar elemental composition (C, H, O, and N) and surface properties (total surface area, pore volume and pore diameter). The positive effects of activation on biochar's HMs adsorption properties suggest that activation is effective for enhancing the remediation of contaminated sites.

4.1. Biochar's HM adsorption depends on the type and mode of activation

Pre-pyrolysis activation being more effective in increasing biochar's HM adsorption capacity, removal efficiency, rate constant, and isotherm constant than post-pyrolysis activation (Table 2) is related to the differential effects of pre- and post-pyrolysis activations on altering biochar's surface structure and adsorption properties (Sizmur et al., 2017; Tan et al., 2016). During pre-pyrolysis activation, agents (such as acids, alkali, metal salts, steam, and radiations) used in activating biochars are introduced onto the

biomass, generating complexes on biochar surfaces; whereas, in post-pyrolysis activation, agents are introduced onto the biochar itself, which may help form new adsorption sites on biochar (Liu et al., 2020). The lower effectiveness of post-pyrolysis activation could be due to the use of corrosive chemicals such as acids and alkali for the activation that might destroy the biochar's mesoporous structure formed during the pyrolysis process and reduce the surface area of the biochar. Moreover, chemicals used in post-pyrolysis activations can also block internal pores and slow the movement of pollutants (such as HMs) toward the interior of the biochar (Tan et al., 2020). Post-pyrolysis activation can also decrease the porosity and surface area, reducing active sites for adsorbing HMs compared to pre-pyrolysis activation.

Our meta-analysis shows that chemical activation enhances biochar's HMs adsorption capacity more effectively than physical activation (Table 2; Fig. 2). Physical activation such as ultrasonication, ball milling, and steam activation specifically alters physical surface properties such as porosity and surface area of biochar (Kazemi Shariat Panahi et al., 2020; Sajjadi et al., 2021), while chemical activation leads to the formation of functional groups such as -NH_2, -OH, and –COOH on biochar surfaces; these functional groups facilitate the adsorption of metals from the solution. The mechanisms underlying the adsorption HMs by biochar are physical adsorption, electrostatic reactions, precipitations, surface complexation, and cation exchange reactions (Inyang et al., 2015; Qiu et al., 2021). However, chemisorption (adsorption mediated via chemical processes) is most often reported as the dominant mechanism for the adsorption process, suggesting that surface functional groups can play a dominant role compared to surface area or porosity in affecting biochar's HM adsorption capacity (Thomas et al., 2020; Wang et al., 2019).

Our meta-analysis shows that metal activations were the most effective among various chemical activations, followed by alkali activations, and acid activations were the least effective method for enhancing biochar's HM adsorption. Biochar activation with metal and alkali load the biochar surface with various functional groups by chelating with organic residues (Medeiros et al., 2022; Wang et al., 2020), making the surface more negatively charged and increasing the surface porosity (Wei et al., 2018). The poor performance of acid-activated biochars can be attributed to their impact on micropore walls, lowering ash content, and enriching surface functional groups with protons. Exposure to acids, for example, could corrode the micropore walls and collapse them, resulting in reduced total surface area and HMs adsorption capability (Sajjadi et al., 2019). Acid activation causes the removal of volatile matter and washes out the inorganic ash present in biochar. Ash contains several minerals and metals that help precipitate HMs on the biochar's surface; thus, washing out ash from biochar can impact its adsorption capability (Peng et al., 2017). All of these factors contribute to influencing biochar's HM adsorption negatively.

4.2. Activation effect on biochar's HM adsorption depends on feedstock type, pyrolysis temperature, and biochar particle size

Activated biochars made from agricultural waste performed better in adsorbing HMs than those produced from woody biomasses can be attributed to the variety and quantity of functional groups associated with different feedstocks. Activated biochars derived from agricultural wastes have more oxygen-containing groups and mineral contents, whereas woody biochars have high aromatic content (Hassan et al., 2020; Jindo et al., 2014). The amount of minerals present corresponds to the adsorption capacity of biochar by changing its pH, active sites, surface morphology, and degradation pathways (Xiao et al., 2017).

The highest adsorption capacity at pyrolysis temperature above 700 °C, followed by 350–550 °C, is related to high pyrolysis temperature decreasing the number of oxygen-containing surface functional groups (that would increase biochar's pH and ash and mineral content) and the cation exchange capacity but increasing the degree of aromatization (Chen et al., 2014) and the biochar's surface area. The enhanced surface area, higher pH, and increasing ash content could favour HM adsorption (Qiu et al., 2021). In contrast to adsorption capacity, the rate constant and isotherm constants for HM adsorption on activated biochar were highest at pyrolysis temperatures of 350–550 °C. The rate constant of biochar measures how fast the equilibrium (basically the completion of the reaction) can be reached. Activated biochars produced at higher temperatures (700 °C) have a lower abundance of functional groups than those produced at a lower temperature (350–550 °C) (Janu et al., 2021). This leads to lesser availability of active sites for chemisorption, and diffusion can become the dominant mechanism.

The effect of activation on biochar's adsorption characteristics with different biochar particle sizes has generally been overlooked in previous studies. We observed that biochar particle size could influence the effect of activation on the adsorption of HMs. The adsorption capacity, rate constant, and isotherm constant were substantially greater in activated biochars with small particle sizes (< 0.25 and 0.25–0.83 mm) as compared to larger particle sizes (>0.83). The total surface area and micropore volume of activated biochars increase with decreasing particle size (Hameed et al., 2020). Particle size does not often impact the type of functional groups. Still, the quantity of functional groups and their exposure to HMs is more significant in the activated biochar with smaller particle sizes (Jin et al., 2022). These enhancements in surface physicochemical properties increase biochar's adsorption capabilities with smaller particle sizes.

4.3. Activation effect on biochar's HM adsorption is dependent on biochar's elemental composition

Biochar's elemental ratios (i.e., N/C, O/C, and H/C) directly influence activated biochar's HM adsorption. The change in aromaticity associated with H/C and hydrophobicity and polarity associated with O/C and (O + N)/C significantly affects biochar's adsorption capacity. Atomic ratios (H/C, O/C, N/C) were traditionally used as international standards for classification. However, the variation in atomic ratios is generally due to the nature of biomass, pyrolysis conditions and, in a few cases, also due to the ageing process. A Higher H/C ratio indicates an increase in the hydrophobicity of biochar, which is not conducive to the adsorption of polar contaminants such as HMs. Higher N/C and O/C ratios indicate the presence of N- and O-containing functional groups (Tan et al., 2016). But our results are somewhat different from these observations; biochars with higher O/C and N/C ratios had a lower increment in HM adsorption after the activation compared to biochars with lower O/C and N/C ratios. One explanation could be that biochars produced at a lower temperature (<400 °C) have the highest amount of N and O functional groups, and with an increase in temperature, the abundance of O and N functional groups decreases (Uchimiya et al., 2011; Zaini et al., 2010). At the same time, biochars produced at higher temperatures had higher ash content and porosity, which play crucial roles in the adsorption process (Shan et al., 2020). This means that biochars produced at a lower temperature can have higher O/C and N/C ratios but lower ash content and porosity, therefore having a lower adsorption potential for HMs. To confirm that biochars having higher O/C, N/C ratios and lower porosity and ash content could have a lower adsorption capacity, we evaluated how O/C and N/C ratios impact the effect of activations on HM adsorption by biochars. We have only included the datasets where biochar was produced at a higher temperature (>400 °C); this is because considering that biochars produced at higher temperatures will have a comparable chemical composition (effect of ash content won't dominate the outcome as most of the biochars would have a similar ash content and surface area). Hence it will help analyze the impact of O/C and N/C ratios on the effect of activation for HM adsorption. However, the effects of O/C and N/C ratios on the impact of activation methods on HM adsorption were not statistically significant (Table S7). Generally, an increase in the N/C ratio signifies higher concentrations of N on the biochar surface, which can enhance the sorption of organic pollutants and the abundance of negatively charged ions (Godwin et al., 2019). A recent study reported that neutral N and O containing functional groups such as -NH_2, -$CONH_2$, tertiary amine (R3N), -OH, C-O-C, and C═O had no interactions with metals. However, most HMs are positively charged;

thus, having higher N/C ratios might not help enhance the adsorption of pollutants (He et al., 2022).

4.4. Activation effect on biochar's HM adsorption depends on biochar surface properties, adsorption contact time and solution pH

The increased adsorption capacity of activated biochar with increasing surface area and surface volume in our meta-analysis is consistent with the literature (Komnitsas et al., 2015; Zhao et al., 2018). It is well established that biochar's porous structure plays a significant role in the adsorption of HMs. During pyrolysis, devolatilization (decomposition of volatile compounds) and dehydration (loss of water molecules) lead to the formation of micropores on the biochar's surface. Most activations aim to increase the surface area, biochar's pore volume and diameter of pore size. Increasing surface area and pore volume provide more active sites on the biochar's surface for the adsorption of pollutants (Islam et al., 2021; Tan et al., 2021). However, the pore size is not directly correlated with adsorption. Depending on the activation method, feedstock type and experimental condition, biochar can have pores of various sizes: nano-pores, mesopores, and macro-pores. In general, activated biochar with smaller pore diameters has more active sites and absorbs more HMs than those with larger pore diameters. However, biochars with a small pore diameter (< 5 nm) cannot capture large adsorbates such as HMs (Shakoor et al., 2019). Adsorption on the activated biochar's surface occurs through film and pore diffusions.

Film diffusion occurs when the metal ions move from the liquid phase to the surface of the adsorbent; then, pore diffusion occurs when the ions move gradually from the biochar surface into the inner surface or pores. This continues till equilibrium is attained (Nzediegwu et al., 2021b; Pathy et al., 2022a). It is important to note that the pore diameter will decide whether the HMs will diffuse from the surface to the inner pores. Thus, too-small pores do not allow larger-sized HMs to enter those pores. This is why the biochars with a pore diameter of <5 nm have a lower adsorption capability than those with a larger pore diameter (5–10 nm). Many activation studies primarily focus on creating meso- and nanoporous structures on biochar surfaces. Thus the choice of activations can impact the porosity of the activated biochar surface and influence HM adsorption.

The highest adsorption of HMs on activated biochar surfaces at pH ranges of 5–8 suggests that extremely low or high pH is not favourable for HM adsorption. At lower pH, the surface functional groups get protonated, which induces electrostatic repulsion between the surface and the adsorbate, resulting in lower adsorption of HMs. However, at higher pH (>8), the HMs precipitate in the solution and become less available for adsorption. Moreover, the optimum pH for the adsorption depends on the HMs, because the speciation of metals (species distribution and their solubility) can vary based on the solution pH (Tan et al., 2016). Our meta-analysis also demonstrated that the adsorption capacity increased with increasing contact time. Although the first step of adsorption, i.e. chemisorption, is a fast process, the second step of adsorption, which involves a diffusion process, is slow. Hence, a longer contact time enables the diffusion process until the maximum extent is reached for HMs adsorption on activated biochar (Islam et al., 2021; Pathy et al., 2022b).

4.5. Activation affects functional groups and biochar HM adsorption

Surface functional groups play an important role in the adsorption of HMs on biochar surfaces. The surface functional groups of biochar determine the types and amounts of HMs that can be absorbed. Various activations have been carried out to load the biochar with functional groups containing oxygen, nitrogen, and sulfur through oxidation, nitrogenation, and sulfuration. Apart from treating the biochar with chemicals, physical activation such as steam activation can load the biochar with oxygen-containing functional groups. The oxygen-containing functional groups have the highest impact on the hydrophilicity, surface reactions, surface behavior, and catalytic and electrical properties of biochar (Yang et al., 2019). These groups were observed to contribute to the adsorption of a wide variety of HMs, including Cd (II), Cr (VI), Hg (II), Ni (II), and Pb (II), onto biochar (Li et al., 2016; Lyu et al., 2018; Tian et al., 2014). Depending on the functional groups, various HM adsorption mechanisms are possible. For instance, oxygen-containing surface groups can form inner-sphere complexes with HMs. Activating biochar with HNO_3 to load the biochar surface with N-containing functional groups helps them to react with HMs and form complex or salt precipitates on the biochar surface (Budaeva and Zoltoev, 2010). Depending on the experimental conditions, sulfur activation of biochar can either increase or decrease surface porosity (Anoop Krishnan and Anirudhan, 2002). The S-containing functional groups have affinities for HMs in the following order: Hg (II) > Pb (II) > Cd (II) > Ni (II). Cu(II), The HMs of Pb(II) and U (VI) can, on the other hand, be absorbed by N-containing groups (Saha et al., 2016). The activation of biochar introduces heteroatoms to biochar surface, allowing biochar to selectively absorb HMs. There is no doubt that the surface functional groups play a major role in the adsorption process; however, it is quite difficult to quantify the surface functional groups; therefore, in our meta-analysis, the impact of activation on the functional groups was not studied.

5. Conclusions

We conclude that the activation of biochar enhances its physicochemical properties and HM adsorption potential. However, not all activation methods equally improve biochar's HMs adsorption, depending on the type and mode of activation that modifies the biochar's properties. Pre-pyrolysis activation is more effective in increasing HM adsorption than post-pyrolysis activation. Similarly, chemical activation performed better than physical activation in increasing biochar's capacity to adsorb HMs. Under chemical activation of biochar, metal salts/oxides and alkali significantly increase HMs adsorption. Our study suggests that the activation effect can be maximized by choosing agricultural waste as the feedstock and producing biochar at a pyrolysis temperature of 350–550 °C. Activation of biochar having smaller particle sizes can adsorb higher amounts of HMs. We also conclude that activating biochars having larger surface area, pore volume, and a moderate pore diameter (5–10 nm) can further enhance the effect of activation. It will be critical to choose the appropriate method of activation, feedstock type and pyrolysis temperature to optimize biochar's physical and chemical properties and enhance the adsorption and removal of HMs from a contaminated environment. In addition to adsorption, various other mechanisms (surface redox reactions, catalytic degradation, and precipitation) might well play a significant role in immobilizing the HMs. Therefore, when evaluating biochar's potential for HMs remediation, it is essential to consider the contributions of these processes and mechanisms. Hence, the activation of biochar can also enhance the other immobilization mechanisms, which were not accounted for in this study.

CRediT authorship contribution statement

Abhijeet Pathy: Conceptualization, Visualization, Data curation, Formal analysis, Investigation, Methodology, Writing – original draft. **Prem Pokhreal:** Conceptualization, Software, Methodology, Writing – review & editing. **Xinli Chen:** Software, Methodology, Writing – review & editing. **Paramasivan Balasubramanian:** Writing – review & editing. **Scott X. Chang:** Conceptualization, Supervision, Writing – review & editing.

Data availability

All the primary data used in this meta-analysis study are available from the corresponding authors upon reasonable request.

Declaration of competing interest

The authors declare that they have no known competing financial interests or personal relationships that could have appeared to influence the work reported in this paper.

Acknowledgement

We are grateful to all the authors whose papers provided the primary data used in this study.

Appendix A. Supplementary data

Supplementary data to this article can be found online at https://doi.org/10.1016/j.scitotenv.2022.161252.

References

Akhil, D., Lakshmi, D., Kartik, A., Vo, D.V.N., Arun, J., Gopinath, K.P., 2021. Production, characterization, activation and environmental applications of engineered biochar: a review. Environmental Chemistry Letters 19 (3), 2261–2297. https://doi.org/10.1007/S10311-020-01167-7 2021 19.

Alver, E., Metin, A.Ü., 2012. Anionic dye removal from aqueous solutions using modified zeolite: adsorption kinetics and isotherm studies. Chemical Engineering Journal 200–202, 59–67. https://doi.org/10.1016/J.CEJ.2012.06.038.

Ambaye, T.G., Vaccari, M., van Hullebusch, E.D., Amrane, A., Rtimi, S., 2020. Mechanisms and adsorption capacities of biochar for the removal of organic and inorganic pollutants from industrial wastewater. International Journal of Environmental Science and Technology 18 (10), 3273–3294. https://doi.org/10.1007/S13762-020-03060-W.

Anon, 2016. Package "boot".

Anoop Krishnan, K., Anirudhan, T.S., 2002. Removal of mercury(II) from aqueous solutions and chlor-alkali industry effluent by steam activated and sulphurised activated carbons prepared from bagasse pith: kinetics and equilibrium studies. J. Hazard. Mater. 92, 161–183. https://doi.org/10.1016/S0304-3894(02)00014-6.

Arabyarmohammadi, H., Darban, A.K., Abdollahy, M., Yong, R., Ayati, B., Zirakjou, A., van der Zee, S.E.A.T.M., 2018. Utilization of a novel Chitosan/Clay/Biochar nanobiocomposite for immobilization of heavy metals in acid soil environment. J. Polym. Environ. 26, 2107–2119. https://doi.org/10.1007/S10924-017-1102-6/TABLES/8.

Bardestani, R., Kaliaguine, S., 2018. Steam activation and mild air oxidation of vacuum pyrolysis biochar. Biomass Bioenergy 108, 101–112. https://doi.org/10.1016/J.BIOMBIOE.2017.10.011.

Barquilha, C.E.R., Braga, M.C.B., 2021. Adsorption of organic and inorganic pollutants onto biochars: challenges, operating conditions, and mechanisms. Bioresour. Technol. Rep. 15, 100728. https://doi.org/10.1016/J.BITEB.2021.100728.

Budaeva, A.D., Zoltoev, E.V., 2010. Porous structure and sorption properties of nitrogen-containing activated carbon. Fuel 89, 2623–2627. https://doi.org/10.1016/J.FUEL.2010.04.016.

Chai, W.S., Cheun, J.Y., Kumar, P.S., Mubashir, M., Majeed, Z., Banat, F., Ho, S.H., Show, P.L., 2021. A review on conventional and novel materials towards heavy metal adsorption in wastewater treatment application. J. Clean. Prod. 296, 126589. https://doi.org/10.1016/J.JCLEPRO.2021.126589.

Chen, T., Zhang, Yaxin, Wang, H., Lu, W., Zhou, Z., Zhang, Yuancheng, Ren, L., 2014. Influence of pyrolysis temperature on characteristics and heavy metal adsorptive performance of biochar derived from municipal sewage sludge. Bioresour. Technol. 164, 47–54. https://doi.org/10.1016/J.BIORTECH.2014.04.048.

Chen, X., Chen, H.Y.H., Chang, S.X., 2022. Meta-analysis shows that plant mixtures increase soil phosphorus availability and plant productivity in diverse ecosystems. Nature Ecology & Evolution 8 (6), 1112–1121. https://doi.org/10.1038/s41559-022-01794-z 2022 6.

Chi, T., Zuo, J., Liu, F., 2017. Performance and mechanism for cadmium and lead adsorption from water and soil by corn straw biochar. Frontiers of Environmental Science & Engineering 2 (11), 1–8. https://doi.org/10.1007/S11783-017-0921-Y 2017 11.

El-Naggar, A., Mosa, A., Ahmed, N., Niazi, N.K., Yousaf, B., Sarkari, B., Rinklebe, J., Cai, Y.J., Chang, S.X., 2022. Modified and pristine biochars for remediation of chromium contamination in soil and aquatic systems. Chemosphere 303 (Part 1), 134942. https://doi.org/10.1016/j.chemosphere.2022.134942.

Essington, M.E., 2015. Soil and water chemistry; an integrative approach. Outlook Agric. 6 298–298.

Fahmi, A.H., Samsuri, A.W., Jol, H., Singh, D., 2018. Physical modification of biochar to expose the inner pores and their functional groups to enhance lead adsorption. RSC Adv. 8, 38270–38280. https://doi.org/10.1039/C8RA06867D.

Gao, Y., Zhu, X., Yue, Q., Gao, B., 2018. Facile one-step synthesis of functionalized biochar from sustainable prolifera-green-tide source for enhanced adsorption of copper ions. J. Environ. Sci. 73, 185–194. https://doi.org/10.1016/J.JES.2018.02.012.

Godwin, P.M., Pan, Y., Xiao, H., Afzal, M.T., 2019. Progress in preparation and application of modified biochar for improving heavy metal ion removal from wastewater. J. Bioresour. Bioprod. 4, 31–42. https://doi.org/10.21967/JBB.V4I1.180.

Greluk, M., Hubicki, Z., 2010. Kinetics, isotherm and thermodynamic studies of reactive black 5 removal by acid acrylic resins. Chem. Eng. J. 162, 919–926. https://doi.org/10.1016/J.CEJ.2010.06.043.

Gupta, S., Babu, B., v., 2009. Utilization of waste product (tamarind seeds) for the removal of Cr(VI) from aqueous solutions: equilibrium, kinetics, and regeneration studies. J. Environ. Manage 90, 3013–3022. https://doi.org/10.1016/J.JENVMAN.2009.04.006.

Gurevitch, J., Koricheva, J., Nakagawa, S., Stewart, G., 2018. Meta-analysis and the science of research synthesis. Nature 7695 (555), 175–182. https://doi.org/10.1038/nature25753 2018 555.

Hameed, R., Lei, C., Lin, D., 2020. Adsorption of organic contaminants on biochar colloids: effects of pyrolysis temperature and particle size. Environ. Sci. Pollut. Res. 27, 18412–18422. https://doi.org/10.1007/S11356-020-08291-5/FIGURES/6.

Hassan, M., Liu, Y., Naidu, R., Parikh, S.J., Du, J., Qi, F., Willett, I.R., 2020. Influences of feedstock sources and pyrolysis temperature on the properties of biochar and functionality as adsorbents: a meta-analysis. Sci. Total Environ. 744, 140714. https://doi.org/10.1016/J.SCITOTENV.2020.140714.

He, M., Xu, Z., Hou, D., Gao, B., Cao, X., Ok, Y.S., Rinklebe, J., Bolan, N.S., Tsang, D.C.W., 2022. Waste-derived biochar for water pollution control and sustainable development. Nat. Rev. Earth Environ. 7 (3), 444–460. https://doi.org/10.1038/s43017-022-00306-8 2017 11.

Inyang, M.I., Gao, B., Yao, Y., Xue, Y., Zimmerman, A., Mosa, A., Pullammanappallil, P., Ok, Y.S., Cao, X., 2015. A Reviewof Biochar as a Low-cost Adsorbent for Aqueous Heavy Metal Removal (doi:10.1080/10643389.2015.1096880 46, 406–433. doi:10.1080/10643389.2015.1096880).

Islam, M.S., Kwak, J.H., Nzediegwu, C., Wang, S., Palansuriya, K., Kwon, E.E., Naeth, M.A., El-Din, M.G., Ok, Y.S., Chang, S.X., 2021. Biochar heavy metal removal in aqueous solution depends on feedstock type and pyrolysis purging gas. Environ. Pollut. 281, 117094. https://doi.org/10.1016/J.ENVPOL.2021.117094.

Janu, R., Mrlik, V., Ribitsch, D., Hofman, J., Sedláček, P., Bielská, L., Soja, G., 2021. Biochar surface functional groups as affected by biomass feedstock, biochar composition and pyrolysis temperature. Carbon Resour. Convers. 4, 36–46. https://doi.org/10.1016/J.CRCON.2021.01.003.

Jin, Z., Xiao, S., Dong, H., Xiao, J., Tian, R., Chen, J., Li, Y., Li, L., 2022. Adsorption and catalytic degradation of organic contaminants by biochar: overlooked role of biochar's particle size. J. Hazard. Mater. 422, 126928. https://doi.org/10.1016/J.JHAZMAT.2021.126928.

Jindo, K., Mizumoto, H., Sawada, Y., Sanchez-Monedero, M.A., Sonoki, T., 2014. Physical and chemical characterization of biochars derived from different agricultural residues. Biogeosciences 11, 6613–6621. https://doi.org/10.5194/BG-11-6613-2014.

Kawi, S., Kathiraser, Y., 2015. CO 2 as an oxidant for high-temperature reactions. Front. Energy Res. 3, 13. https://doi.org/10.3389/FENRG.2015.00013/BIBTEX.

Kazemi Shariat Panahi, H., Dehhaghi, M., Ok, Y.S., Nizami, A.S., Khoshnevisan, B., Mussatto, S.I., Aghbashlo, M., Tabatabaei, M., Lam, S.S., 2020. A comprehensive review of engineered biochar: production, characteristics, and environmental applications. J Clean Prod 270, 122462. https://doi.org/10.1016/J.JCLEPRO.2020.122462.

Komnitsas, K., Zaharaki, D., Pyliotis, I., Vamvuka, D., Bartzas, G., 2015. Assessment of pistachio shell biochar quality and its potential for adsorption of heavy metals. Waste Biomass Valoriz. 6 (5), 805–816.

Leng, L., Xiong, Q., Yang, L., Li, Hui, Zhou, Y., Zhang, W., Jiang, S., Li, Hailong, Huang, H., 2021. An overview on engineering the surface area and porosity of biochar. Sci. Total Environ. 763, 144204. https://doi.org/10.1016/J.SCITOTENV.2020.144204.

Li, F., Wang, X., Yuan, T., Sun, R., 2016. A lignosulfonate-modified graphene hydrogel with ultrahigh adsorption capacity for Pb(II) removal. J. Mater. Chem. A Mater. 4, 11888–11896. https://doi.org/10.1039/C6TA03779H.

Li, B., Yang, L., Wang, C.Quan, Zhang, Q.Pei, Liu, Q.Cheng, Li, Y.Ding, Xiao, R., 2017. Adsorption of Cd(II) from aqueous solutions by rape straw biochar derived from different modification processes. Chemosphere 175, 332–340. https://doi.org/10.1016/J.CHEMOSPHERE.2017.02.061.

Liu, Z., Dugan, B., Masiello, C.A., Gonnermann, H.M., 2017. Biochar particle size, shape, and porosity act together to influence soil water properties. PLoS One 12, e0179079. https://doi.org/10.1371/JOURNAL.PONE.0179079.

Liu, J., Yang, X., Liu, H., Cheng, W., Bao, Y., 2020. Modification of calcium-rich biochar by loading Si/Mn binary oxide after NaOH activation and its adsorption mechanisms for removal of Cu(II) from aqueous solution. Colloids Surf. A Physicochem. Eng. Asp. 601, 124960. https://doi.org/10.1016/J.COLSURFA.2020.124960.

Luo, Y., Hui, D., Zhang, D., 2006. Elevated CO2 stimulates net accumulations of carbon and nitrogen in land ecosystems: a meta-analysis. Ecology 87 (1), 53–63.

Luo, M., Lin, H., Li, B., Dong, Y., He, Y., Wang, L., 2018. A novel modification of lignin on corncob-based biochar to enhance removal of cadmium from water. Bioresour. Technol. 259, 312–318. https://doi.org/10.1016/J.BIORTECH.2018.03.075.

Lyu, H., Gao, B., He, F., Zimmerman, A.R., Ding, C., Huang, H., Tang, J., 2018. Effects of ball milling on the physicochemical and sorptive properties of biochar: experimental observations and governing mechanisms. Environ. Pollut. 233, 54–63. https://doi.org/10.1016/J.ENVPOL.2017.10.037.

Ma, Z., Chen, H.Y.H., 2016. Effects of species diversity on fine root productivity in diverse ecosystems: a global meta-analysis. Glob. Ecol. Biogeogr. 25, 1387–1396. https://doi.org/10.1111/GEB.12488.

Mahdi, Z., el Hanandeh, A., Yu, Q.J., 2019. Preparation, characterization and application of surface modified biochar from date seed for improved lead, copper, and nickel removal from aqueous solutions. J. Environ. Chem. Eng. 7, 103379. https://doi.org/10.1016/J.JECE.2019.103379.

Mariana, M., Abdul, A.K., Mistar, E.M., Yahya, E.B., Alfatah, T., Danish, M., Amayreh, M., 2021. Recent advances in activated carbon modification techniques for enhanced heavy metal adsorption. J. Water Process Eng. 43, 102221. https://doi.org/10.1016/J.JWPE.2021.102221.

Medeiros, D.C.C.da S., Nzediegwu, C., Benally, C., Messele, S.A., Kwak, J.H., Naeth, M.A., Ok, Y.S., Chang, S.X., Gamal El-Din, M., 2022. Pristine and engineered biochar for the removal of contaminants co-existing in several types of industrial wastewaters: a critical review. Science of The Total Environment 809, 151120. https://doi.org/10.1016/J.SCITOTENV.2021.151120.

Mikolajewicz, N., Komarova, S.V., 2019. Meta-analytic methodology for basic research: a practical guide. Front Physiol 10, 203. https://doi.org/10.3389/FPHYS.2019.00203/BIBTEX.

Nzediegwu, C., Arshad, M., Ulah, A., Naeth, M.A., Chang, S.X., 2021a. Fuel, thermal and surface properties of microwave-pyrolyzed biochars depend on feedstock type and pyrolysis temperature. Bioresour. Technol. 320, 124282. https://doi.org/10.1016/J.BIORTECH.2020.124282.

Nzediegwu, C., Naeth, M.A., Chang, S.X., 2021b. Lead(II) adsorption on microwave-pyrolyzed biochars and hydrochars depends on feedstock type and production temperature. J. Hazard. Mater. 412, 125255. https://doi.org/10.1016/J.JHAZMAT.2021.125255.

Ore, O.T., Adeola, A.O., 2021. Toxic metals in oil sands: review of human health implications, environmental impact, and potential remediation using membrane-based approach. Energy Ecol. Environ. 6, 81–91. https://doi.org/10.1007/S40974-020-00196-W/TABLES/3.

Pathy, A., Krishnamoorthy, N., Chang, S.X., Paramasivan, B., 2022a. Malachite green removal using algal biochar and its composites with kombucha SCOBY: an integrated biosorption and phycoremediation approach. Surf. Interfaces 30, 101880. https://doi.org/10.1016/J.SURFIN.2022.101880.

Pathy, A., Krishnamoorthy, N., Chang, S.X., Paramasivan, B., 2022b. Malachite green removal using algal biochar and its composites with kombucha SCOBY: an integrated biosorption and phycoremediation approach. Surf. Interfaces 30, 101880. https://doi.org/10.1016/J.SURFIN.2022.101880.

Peng, H., Gao, P., Chu, G., Pan, B., Peng, J., Xing, B., 2017. Enhanced adsorption of Cu(II) and Cd(II) by phosphoric acid-modified biochars. Environ. Pollut. 229, 846–853. https://doi.org/10.1016/J.ENVPOL.2017.07.004.

Pokharel, P., Ma, Z., Chang, S.X., 2020. Biochar increases soil microbial biomass with changes in extra- and intracellular enzyme activities: a global meta-analysis. Biochar 1 (2), 65–79. https://doi.org/10.1007/S42773-020-00039-1 2020 2.

Qiu, B., Tao, X., Wang, H., Li, W., Ding, X., Chu, H., 2021. Biochar as a low-cost adsorbent for aqueous heavy metal removal: a review. J. Anal. Appl. Pyrolysis 155, 105081. https://doi.org/10.1016/J.JAAP.2021.105081.

Rajendran, S., Priya, T.A.K., Khoo, K.S., Hoang, T.K.A., Ng, H.S., Munawaroh, H.S.H., Karaman, C., Orooji, Y., Show, P.L., 2022. A critical review on various remediation approaches for heavy metal contaminants removal from contaminated soils. Chemosphere 287, 132369. https://doi.org/10.1016/J.CHEMOSPHERE.2021.132369.

Saha, D., Barakat, S., van Bramer, S.E., Nelson, K.A., Hensley, D.K., Chen, J., 2016. Noncompetitive and competitive adsorption of heavy metals in sulfur-functionalized ordered mesoporous carbon. ACS Appl. Mater. Interfaces 8, 34132–34142. https://doi.org/10.1021/ACSAMI.6B12190/ASSET/IMAGES/LARGE/AM-2016-12190D_0011.JPEG.

Sajjadi, B., Zubatiuk, T., Leszczynska, D., Leszczynski, J., Chen, W.Y., 2019. Chemical activation of biochar for energy and environmental applications: a comprehensive review. Rev. Chem. Eng. 35, 777–815. https://doi.org/10.1515/REVCE-2018-0003/XML.

Sajjadi, B., Shrestha, R.M., Chen, W.Y., Mattern, D.L., Hammer, N., Raman, V., Dorris, A., 2021. Double-layer magnetized/functionalized biochar composite: role of microporous structure for heavy metal removals. v 39, 101677. https://doi.org/10.1016/J.JWPE.2020.101677.

Shakoor, M.B., Ali, S., Rizwan, M., Abbas, F., Bibi, I., Riaz, M., Khalil, U., Niazi, N.K., Rinklebe, J., 2019. A Reviewof Biochar-based Sorbents for Separation of Heavy Metals From Water. 22, pp. 111–126. https://doi.org/10.1080/15226514.2019.1647405.

Shan, R., Shi, Y., Gu, J., Wang, Y., Yuan, H., 2020. Single and competitive adsorption affinity of heavy metals toward peanut shell-derived biochar and its mechanisms in aqueous systems. Chin. J. Chem. Eng. 28, 1375–1383. https://doi.org/10.1016/J.CJCHE.2020.02.012.

Sizmur, T., Fresno, T., Akgül, G., Frost, H., Moreno-Jiménez, E., 2017. Biochar modification to enhance sorption of inorganics from water. Bioresour. Technol. 246, 34–47. https://doi.org/10.1016/J.BIORTECH.2017.07.082.

Tan, G., Sun, W., Xu, Y., Wang, H., Xu, N., 2016. Sorption of mercury (II) and atrazine by biochar, modified biochars and biochar based activated carbon in aqueous solution. Bioresour. Technol. 211, 727–735. https://doi.org/10.1016/J.BIORTECH.2016.03.147.

Tan, G., Mao, Y., Wang, H., Xu, N., 2020. A comparative study of arsenic(V), tetracycline and nitrate ions adsorption onto magnetic biochars and activated carbon. Chem. Eng. Res. Des. 159, 582–591. https://doi.org/10.1016/J.CHERD.2020.05.011.

Tan, X.F., Zhu, S.S., Wang, R.P., Chen, Y.Di, Show, P.L., Zhang, F.F., Ho, S.H., 2021. Role of biochar surface characteristics in the adsorption of aromatic compounds: pore structure and functional groups. Chin. Chem. Lett. 32, 2939–2946. https://doi.org/10.1016/J.CCLET.2021.04.059.

Thomas, E., Borchard, N., Sarmiento, C., Atkinson, R., Ladd, B., 2020. Key factors determining biochar sorption capacity for metal contaminants: a literature synthesis. Biochar 2, 151–163. https://doi.org/10.1007/S42773-020-00053-3/TABLES/3.

Tian, Z., Yang, B., Cui, G., Zhang, L., Guo, Y., Yan, S., 2014. Synthesis of poly(m-phenylenediamine)/iron oxide/acid oxidized multi-wall carbon nanotubes for removal of hexavalent chromium. RSC Adv. 5, 2266–2275. https://doi.org/10.1039/C4RA10282G.

Uchimiya, M., Wartelle, L.H., Klasson, K.T., Fortier, C.A., Lima, I.M., 2011. Influence of pyrolysis temperature on biochar property and function as a heavy metal sorbent in soil. J. Agric. Food Chem. 59, 2501–2510. https://doi.org/10.1021/jf104206c.

Wang, L., Wang, Y., Ma, F., Tankpa, V., Bai, S., Guo, X., Wang, X., 2019. Mechanisms and reutilization of modified biochar used for removal of heavy metals from wastewater: a review. Sci. Total Environ. 668, 1298–1309. https://doi.org/10.1016/J.SCITOTENV.2019.03.011.

Wang, S., Kwak, J.H., Islam, M.S., Naeth, M.A., Gamal El-Din, M., Chang, S.X., 2020. Biochar surface complexation and Ni(II), Cu(II), and Cd(II) adsorption in aqueous solutions depend on feedstock type. Sci. Total Environ. 712, 136538. https://doi.org/10.1016/j.scitotenv.2020.136538.

Wei, D., Ngo, H.H., Guo, W., Xu, W., Du, B., Khan, M.S., Wei, Q., 2018. Biosorption performance evaluation of heavy metal onto aerobic granular sludge-derived biochar in the presence of effluent organic matter via batch and fluorescence approaches. Bioresour. Technol. 249, 410–416. https://doi.org/10.1016/J.BIORTECH.2017.10.015.

Wiernik, B.M., Dahlke, J.A., 2020. Obtaining Unbiased Results in Meta-Analysis: The Importance of Correcting for Statistical Artifacts. 3, pp. 94–123. https://doi.org/10.1177/2515245919885611.

Wu, W., Li, J., Niazi, N.K., Müller, K., Chu, Y., Zhang, L., Yuan, G., Lu, K., Song, Z., Wang, H., 2016. Influence of pyrolysis temperature on lead immobilization by chemically modified coconut fiber-derived biochars in aqueous environments. Environ. Sci. Pollut. Res. 23, 22890–22896. https://doi.org/10.1007/S11356-016-7428-0/FIGURES/2.

Xiao, Y., Xue, Y., Gao, F., Mosa, A., 2017. Sorption of heavy metal ions onto crayfish shell biochar: effect of pyrolysis temperature, pH and ionic strength. J. Taiwan Inst. Chem. Eng. 80, 114–121. https://doi.org/10.1016/J.JTICE.2017.08.035.

Xu, Z., Wan, Z., Sun, Y., Gao, B., Hou, D., Cao, X., Komárek, M., Ok, Y.S., Tsang, D.C.W., 2022. Electroactive fe-biochar for redox-related remediation of arsenic and chromium: distinct redox nature with varying iron/carbon speciation. J. Hazard. Mater. 430, 128479. https://doi.org/10.1016/J.JHAZMAT.2022.128479.

Yang, X., Wan, Y., Zheng, Y., He, F., Yu, Z., Huang, J., Wang, H., Ok, Y.S., Jiang, Y., Gao, B., 2019. Surface functional groups of carbon-based adsorbents and their roles in the removal of heavy metals from aqueous solutions: a critical review. Chem. Eng. J. 366, 608–621. https://doi.org/10.1016/J.CEJ.2019.02.119.

Yuvaraj, A., Thangaraj, R., Karmegam, N., Ravindran, B., Chang, S.W., Awasthi, M.K., Kannan, S., 2021. Activation of biochar through exoenzymes prompted by earthworms for vermibiochar production: a viable resource recovery option for heavy metal contaminated soils and water. Chemosphere 278, 130458. https://doi.org/10.1016/J.CHEMOSPHERE.2021.130458.

Zaini, M.A.A., Amano, Y., Machida, M., 2010. Adsorption of heavy metals onto activated carbons derived from polyacrylonitrile fiber. J. Hazard. Mater. 180, 552–560. https://doi.org/10.1016/J.JHAZMAT.2010.04.069.

Zamora-Ledezma, C., Negrete-Bolagay, D., Figueroa, F., Zamora-Ledezma, E., Ni, M., Alexis, F., Guerrero, V.H., 2021. Heavy metal water pollution: a fresh look about hazards, novel and conventional remediation methods. Environ. Technol. Innov. 22, 101504. https://doi.org/10.1016/J.ETI.2021.101504.

Zhang, L., Jing, Y., Xiang, Y., Zhang, R., Lu, H., 2018. Responses of soil microbial community structure changes and activities to biochar addition: a meta-analysis. Sci. Total Environ. 643, 926–935. https://doi.org/10.1016/J.SCITOTENV.2018.06.231.

Zhang, X., Zhang, L., Li, A., 2018. Eucalyptus sawdust derived biochar generated by combining the hydrothermal carbonization and low concentration KOH modification for hexavalent chromium removal. J. Environ. Manag. 206, 989–998. https://doi.org/10.1016/J.JENVMAN.2017.11.079.

Zhao, B., Xu, X., Zeng, F., Li, H., Chen, X., 2018. The hierarchical porous structure bio-char assessments produced by co-pyrolysis of municipal sewage sludge and hazelnut shell and Cu (II) adsorption kinetics. Environ. Sci. Pollut. Res. 25 (20), 19423–19435.